

# IEICE Proceeding Series

Hierarchical Transition Chronometries in the Human Central Nervous System

Paul E. Rapp, David M. Darmon, Christopher J. Cellucci

Vol. 2 pp. 286-289

Publication Date: 2014/03/18

Online ISSN: 2188-5079

Downloaded from [www.proceeding.ieice.org](http://www.proceeding.ieice.org)

## Hierarchical Transition Chronometries in the Human Central Nervous System

Paul E. Rapp\*, David M. Darmon<sup>†</sup> and Christopher J. Cellucci<sup>‡</sup>

\*Uniformed Services University, 4301 Jones Bridge Road, Bethesda, MD

<sup>†</sup>Department of Mathematics, University of Maryland, College Park, MD

<sup>‡</sup>Aquinas, LLC, 2014 St. Andrews Drive, Berwyn, PA

Alterations of functional central nervous system networks occur as the result of traumatic brain injury. Characterization of functional network structure is therefore an essential element in the initial evaluation of these patients and in the longitudinal assessment of the response to treatment. Several methods of dynamical analysis have been used to quantify CNS reorganization during recovery. They include measures of inter-regional synchronization, analysis of network geometries (small world models) and the identification of causal networks. This project began with the identification of causal networks as its objective. This form of analysis moves beyond correlation by quantifying the direction and magnitude of information flow. An immediate difficulty presented itself. Consider a simple network consisting of two channels, Channel A and Channel B. Suppose that from time  $t_0$  to  $t_1$  Channel A is a strong causal driver of Channel B, and suppose further that from time  $t_1$  to  $t_2$  Channel B drives Channel A. If a causal analysis is constructed over the temporal epoch  $t_0$  to  $t_2$ , a failure to detect any causal relationships will probably result. It follows that an identification of transition chronometry is the first step in causality analysis. There are several classes of mathematical technologies for identifying transitions. Here we consider methods based on the examination of embedded data.

Let  $\{x_1, x_2, \dots, x_N\}$  be a scalar time series recorded with a uniform sampling interval of  $\Delta t$ . These data are used to construct a set of points

$$\{Z_k\} \in \mathfrak{R}^m$$

$$Z_k = (x_k, x_{k+L}, x_{k+2L}, \dots, x_{k+(m-1)L})$$

Parameter  $m$  is the embedding dimension and  $L$  is the lag. The window is the temporal epoch spanned by a

single point with a length given by  $(m-1)L\Delta t$ . For point  $Z_i$  in the embedding space, the corresponding time  $t_i$  is the midpoint of the temporal epoch spanned from  $x_i$  at time  $(i-1)\Delta t$  to  $x_{i+(m-1)L}$  at time  $(i+(m-1)L-1)\Delta t$ . The original time series has now become a trajectory in  $\mathfrak{R}^m$ ,  $Z_1 \rightarrow Z_2 \rightarrow Z_3 \rightarrow \dots$

Embedding is motivated by the Takens embedding theorem (Takens, 1980). Stated informally, suppose that the observed signal is generated by a dynamical system  $\Psi$  of  $\omega$  real variables not all of which are observable. If the conditions of the theorem are met, then properties of the continuous extension map  $Z_j \rightarrow Z_{j+1}$  will, up to a diffeomorphism, be true of  $\Psi$ . It should be stressed that the conditions of the theorem will never be satisfied with a finite data set, but experience with simple model systems does suggest that  $Z_j \rightarrow Z_{j+1}$  can sometimes be informative about the dynamical behavior of  $\Psi$ . A model based on an embedding is in a mathematical sense minimally restrictive. It only assumes that  $\Psi$  is a finite dimensional dynamical system on a compact behavior space. It is mechanistically agnostic and offers the possibility of examining the behavior of a large dimensional system with a limited number of observed variables.

Transition behavior in  $Z_j \rightarrow Z_{j+1}$  was examined by constructing two dimensional recurrence plots (Eckmann, Kamphorst and Ruelle, 1987). The construction starts by finding the nearest neighbors of each point in the embedding space. The number of nearest neighbors used is a parameter of the construction. For example, suppose that ten nearest neighbors are used and that the nearest

neighbors of  $Z_{27}$  are  $Z_{26}$ ,  $Z_{28}$ ,  $Z_{24}$ ,  $Z_{30}$ ,  $Z_1$ ,  $Z_{17}$ ,  $Z_{204}$ ,  $Z_{203}$ ,  $Z_{19}$  and  $Z_{423}$ . The following points are plotted on the diagram: (27,26), (27,28), (27,24), (27,30), (27,1), (27,17), (27,204), (27, 203), (27,19) and (27,423). The recurrence diagram may be thought of as an  $N_\varepsilon \times N_\varepsilon$  directed adjacency matrix, where adjacency is determined by the nearest neighbor relationship and  $N_\varepsilon$  is the number of embedded points. The recurrence diagram is completed by finding the nearest neighbors for each embedded point and filling in this adjacency matrix. Eckmann, et al. found that visual examination of the recurrence plot could discover transitions in dynamical behavior that were not found by direct examination of the original time series. An example where the transition is readily apparent in the time series is shown in the first diagram. The signal is a single channel EEG recorded at 1 KHz in a rat. The transition at approximately  $t=1.1$  seconds is a transition from a tonic to a clonic seizure. The corresponding recurrence plot is shown on the bottom side of the diagram. We wanted to find a way of quantifying the transition structure that was visually identifiable in the recurrence diagram

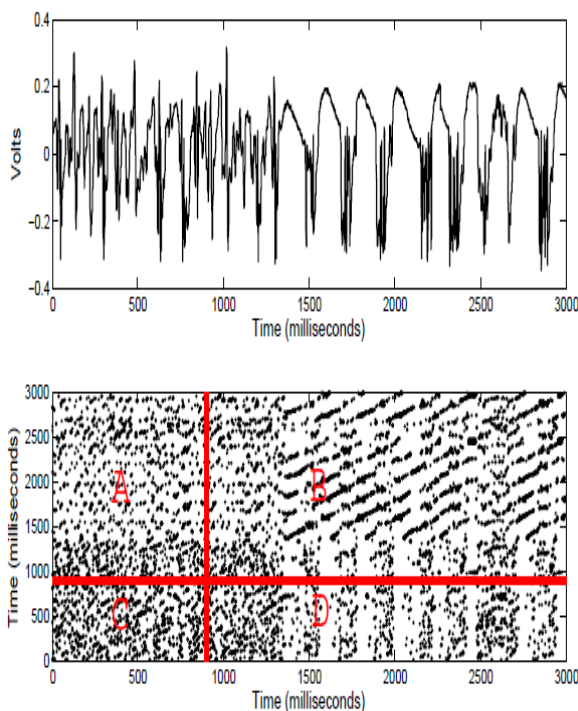


Figure 1 (A) An EEG recorded at 1 KHz in a rat. (B) The corresponding recurrence diagram for embedding dimension  $m=5$ ,  $Lag=1$  and five nearest neighbors.

A quadrant scan is a continuous function of time derived from a recurrence diagram that quantifies the geometrical relationship between a dynamical system's past and future. (To clarify, the quadrant scan is continuous in that it has the same sampling interval as the original time series.) Consider an arbitrary point  $Z_i$  and its corresponding time  $t_i$ . A vertical line at  $t_i$  and a horizontal line at  $t_i$  divides the recurrence diagram into four quadrants. The points in Quadrant A are neighbors of points in  $Z_i$ 's past (they are to the left of the vertical line) that are in  $Z_i$ 's future (they are above the horizontal line). Neighbors of past points that are in  $Z_i$ 's future result when the trajectory of the dynamical system folds back on itself. They are, in this sense, irregular. In contrast, points in Quadrant B are neighbors of points in  $Z_i$ 's future that are also in  $Z_i$ 's future. We describe them as being regular. Similarly points in Quadrants C and D are regular and irregular respectively. To summarize:

Quadrant A. Neighbors of points in  $Z_i$ 's past that are in  $Z_i$ 's future, Irregular Points

Quadrant B. Neighbors of points in  $Z_i$ 's future that are also in  $Z_i$ 's future, Regular Points

Quadrant C. Neighbors of points in  $Z_i$ 's past that are also in  $Z_i$ 's past, Regular Points

Quadrant D. Neighbors of points in  $Z_i$ 's future that are in  $Z_i$ 's past, Irregular Points.

A quadrant scan quantifies the relative density of regular and irregular points as a function of time. Let  $N_A$  be the number of occupied nodes in Quadrant A. Let  $N_{NA}$  be the total number of nodes in Quadrant A. Analogous variables are defined for Quadrants B, C and D. For any given point  $Z_i$  corresponding to time  $t_i$ , quadrant scan  $Q(t_i)$  is defined by

$$Q(t_i) = \frac{\left( \frac{N_B + N_C}{N_{NB} + N_{NC}} \right)}{\left( \frac{N_B + N_C}{N_{NB} + N_{NC}} \right) + \left( \frac{N_A + N_D}{N_{NA} + N_{ND}} \right)}$$

The interpretation of a quadrant scan is best introduced by considering a time series that contains a single dramatic transition. The time series is shown in the top panel of Figure 2. It is a sine wave that makes a transition from a baseline of -2 to a baseline of +2 at  $t=500$ . The corresponding recurrence diagram is shown in the center panel, and the quadrant scan is shown in the bottom panel. The relative density of regular points decreases at a transition. Local maxima of quadrant scans identify transitions.

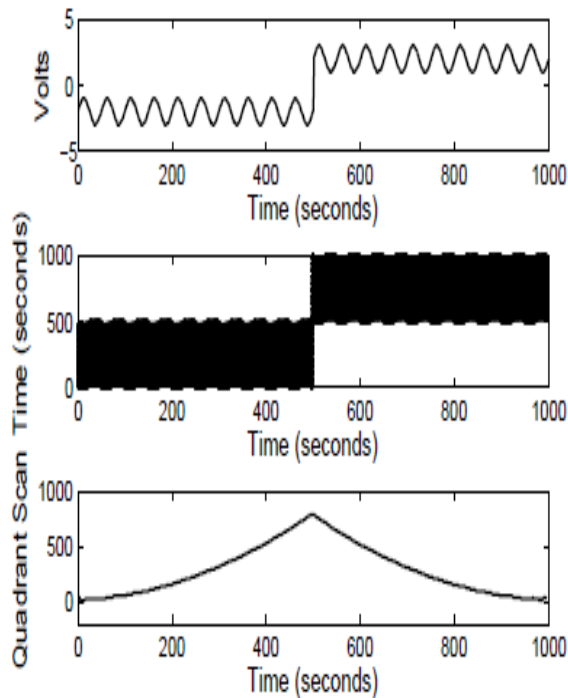


Figure 2 (A) The time series: a sine wave making a transition. (B) The recurrence diagram for  $m=5$ ,  $L=1$  and one hundred nearest neighbors. (C) The quadrant scan

The sensitivity of the quadrant scan to embedding parameters is instructive. Figure 3 shows quadrant scans for the EEG signal for  $m=10$  and  $L=1, 2, 10, 20$  and  $30$ . These embeddings correspond to temporal windows of 9, 18, 90, 180 and 270 milliseconds. Transitions not apparent in quadrant

scans at larger time scales appear at smaller time scales.

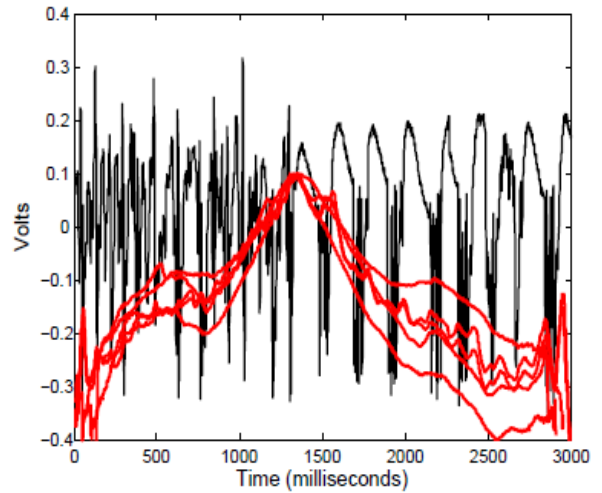


Figure 3. The original time series and the superimposed quadrant scans for one hundred nearest neighbors,  $m=10$  and  $L=1, 2, 10, 20$  and  $30$ .

An examination of Figure 3 leads to an open question. Can the dependence of local maxima of quadrant scans on the embedding window be used to quantify hierarchical transition behavior in the central nervous system? The idea of a hierarchy of time scales in the CNS has a long history and has recently received increased attention (Kiebel, et al., 2008; Perdakis, et al., 2011; Papo, 2013). A means of providing a systematic quantitative structure to this concept may be available by expressing CNS chronometry as a function of embedding window. We also note that the quadrant scan is a continuous function of time; that is, it has the same sampling interval as the original time series. Therefore change point detection technologies applied to time series, for example piecewise regression models (Hawkins, 1976), hierarchical Bayesian analysis (Carter, et al., 1994) and maximum likelihood methods (Guralnik and Srivastava, 1999), can be applied to quadrant scans. We can use the statistical tests of earlier methods to characterize the dynamical structures revealed by embedding.

### Acknowledgments

We acknowledge support from the Uniformed Services University, the Marine Corps Systems Command and the Defense Medical Research and Development Program. We thank Professor Norman Kreisman, Tulane University for the EEG record. The opinions and assertions contained herein are the

personal opinions of the authors and are not to be construed as official or reflecting the views of the United States Department of Defense.

C. K. Carter and R. Kohn, "On Gibbs sampling for state space models," *Biometrika*. 81, 541-553, 1994.

V. Guralnik and J. Srivastava, "Event detection from time series data," *Proceedings Fifth ACM SIGKDD International Conference on Knowledge Discovery and Data Mining*. San Diego, CA. pp. 33-42, 1999.

D. M. Hawkins, "Point estimation of the parameters of piecewise regression models," *Applied Statistics*. 25(1), 51-57, 1976.

S. J. Kiebel, S. J. Daunizeau and K. J. Friston, "A hierarchy of time scales in the brain," *PLoS Computational Biology*. 4(11), e1000209, 2008.

D. Papo, "Time scales in cognitive neuroscience." *Frontiers in Physiology*, 4, 86, 2013.

D. Perdikis, R. Huys and V. Jirsa, "Complex processes from dynamical architectures with time-scale hierarchy," *PLoS One*. 6(2), e16589, 2011.

F. Takens, "Detecting strange attractors in turbulence," *Lecture Notes in Mathematics*. Volume 898. D. A. Rand and L. S. Young, eds. pp. 365-381. Springer-Verlag, NY, 1980.